

NUMERICAL SIMULATION OF MUD FLOW GENERATED IN ATSUMA, HOKKAIDO, JAPAN

ARATA ISHIKAWA

Kyoto University Graduate School of Engineering, Kyoto, Japan, ishikawa.arata.56z@st.kyoto-u.ac.jp

HIROSHI TAKEBAYASHI

Kyoto University, Kyoto, Japan, takebayashi.hiroshi.6s@kyoto-u.ac.jp

MASAHARU FUJITA

Kyoto University, Kyoto, Japan, fujita.masaharu.5x@kyoto-u.ac.jp

ABSTRACT

In Atsuma, Hokkaido, mud flow occurred due to the 2018 Hokkaido Eastern Iburi Earthquake. In this study, numerical simulation of the mud flow is conducted to discuss its flow characteristics. The governing equations on the bases of the two-dimensional continuum body model are used in the numerical analysis. Results showed that the depth averaged velocity of the mud flowing down the slope is 13.5 m/s and the depth of the mud flow when reaching the house is about 6 m. The mud flow spread over farmland widely. The mud flow reaches the house in about 6 seconds. It is impossible for residents living at the bottom of the slope to evacuate, because the mud flow originated from the earthquake, and 6 seconds is too short to evacuate. Therefore, it is important to avoid as much as possible to build houses near slopes with topsoil composed of fine-grained pyroclastic fall materials with high moisture retention.

Keywords: Mud flow, Earthquake, Acceleration, Evacuation, Numerical simulation

1. INTRODUCTION

On September 6, 2018, "Hokkaido Eastern Iburi Earthquake" (magnitude 6.7) occurred at a depth of about 35 km in the central eastern Hokkaido Iburi district. The earthquake caused 223 debris flows, landslides and other sediment disasters, causing 36 people to die and 470 buildings to be completely or partially destroyed by this disaster. The damage caused by sediment disaster to humans is enormous. In this study, numerical analysis model of mud flow on the bases of the two-dimensional continuum body model was developed and numerical simulation of the mud flow occurred due to the 2018 Hokkaido Eastern Iburi Earthquake is conducted to discuss its flow characteristics. By using the numerical model, damages from mud flow can be predicted, and simulation results can be used for making evacuation plan.

2. NUMERICAL SIMULATION MODEL

2.1 Numerical analysis method

Numerical simulation of mudflow is carried out in the Yoshino area to study the flow characteristics of the mud flow. Slope failures occur continuously in the cross-slope direction, but it is not clear whether the slope failures occurred simultaneously at all locations. In this study, a slender shape landslide, that crosses the slope, is used and performed numerical simulation under the condition that the slope collapse occurred at all places at the same time. It is assumed that the mixture of water and soil quickly became muddy due to the oscillation of the earthquake and flowed down the slope. The depth of the slope failure was determined based on the difference between the DSM ground height measured by a drone and the DEM measured by GSI before the disaster. Except for the momentum conservation equations, the basic equations used in the analysis are the same as the two-dimensional mudflow analysis model of Takebayashi and Fujita (2020). The equation of motion of the mudflow considering the seismic acceleration is described as follows in general coordinate system.

$$\begin{aligned} & \frac{\partial}{\partial t} \left(\frac{hU}{J} \right) + \frac{\partial}{\partial \xi} \left(U \frac{hU}{J} \right) + \frac{\partial}{\partial \eta} \left(V \frac{hU}{J} \right) - \frac{hu}{J} \left(U \frac{\partial}{\partial \xi} \left(\frac{\partial \xi}{\partial x} \right) + V \frac{\partial}{\partial \eta} \left(\frac{\partial \xi}{\partial x} \right) \right) - \frac{hv}{J} \left(U \frac{\partial}{\partial \xi} \left(\frac{\partial \xi}{\partial y} \right) + V \frac{\partial}{\partial \eta} \left(\frac{\partial \xi}{\partial y} \right) \right) \\ & = -(g - a_z)h \left(\frac{1}{J} \left(\left(\frac{\partial \xi}{\partial x} \right)^2 + \left(\frac{\partial \xi}{\partial y} \right)^2 \right) \frac{\partial z_b}{\partial \xi} + \frac{1}{J} \left(\frac{\partial \xi}{\partial x} \frac{\partial \eta}{\partial x} + \frac{\partial \xi}{\partial y} \frac{\partial \eta}{\partial y} \right) \frac{\partial z_b}{\partial \eta} \right) + a_\xi \frac{h}{J} \cos \theta \\ & \quad - \frac{1}{\rho_m} \left(\frac{1}{J} \left(\left(\frac{\partial \xi}{\partial x} \right)^2 + \left(\frac{\partial \xi}{\partial y} \right)^2 \right) \frac{\partial P}{\partial \xi} + \frac{1}{J} \left(\frac{\partial \xi}{\partial x} \frac{\partial \eta}{\partial x} + \frac{\partial \xi}{\partial y} \frac{\partial \eta}{\partial y} \right) \frac{\partial P}{\partial \eta} \right) - \frac{\tau_{b\xi}}{\rho_m J} \end{aligned} \quad (1)$$

$$\begin{aligned}
& \frac{\partial}{\partial t} \left(\frac{hV}{J} \right) + \frac{\partial}{\partial \xi} \left(U \frac{hV}{J} \right) + \frac{\partial}{\partial \eta} \left(V \frac{hV}{J} \right) - \frac{hu}{J} \left(U \frac{\partial}{\partial \xi} \left(\frac{\partial \eta}{\partial x} \right) + V \frac{\partial}{\partial \eta} \left(\frac{\partial \eta}{\partial x} \right) \right) - \frac{hv}{J} \left(U \frac{\partial}{\partial \xi} \left(\frac{\partial \eta}{\partial y} \right) + V \frac{\partial}{\partial \eta} \left(\frac{\partial \eta}{\partial y} \right) \right) \\
& = -(g - a_z)h \left(\frac{1}{J} \left(\frac{\partial \xi}{\partial x} \frac{\partial \eta}{\partial x} + \frac{\partial \xi}{\partial y} \frac{\partial \eta}{\partial y} \right) \frac{\partial z_b}{\partial \xi} + \frac{1}{J} \left(\left(\frac{\partial \eta}{\partial x} \right)^2 + \left(\frac{\partial \eta}{\partial y} \right)^2 \right) \frac{\partial z_b}{\partial \eta} \right) + a_\eta \frac{h}{J} \cos \theta \\
& \quad - \frac{1}{\rho_m} \left(\frac{1}{J} \left(\frac{\partial \xi}{\partial x} \frac{\partial \eta}{\partial x} + \frac{\partial \xi}{\partial y} \frac{\partial \eta}{\partial y} \right) \frac{\partial P}{\partial \xi} + \frac{1}{J} \left(\left(\frac{\partial \eta}{\partial x} \right)^2 + \left(\frac{\partial \eta}{\partial y} \right)^2 \right) \frac{\partial P}{\partial \eta} \right) - \frac{\tau_{b\eta}}{\rho_m J}
\end{aligned} \tag{2}$$

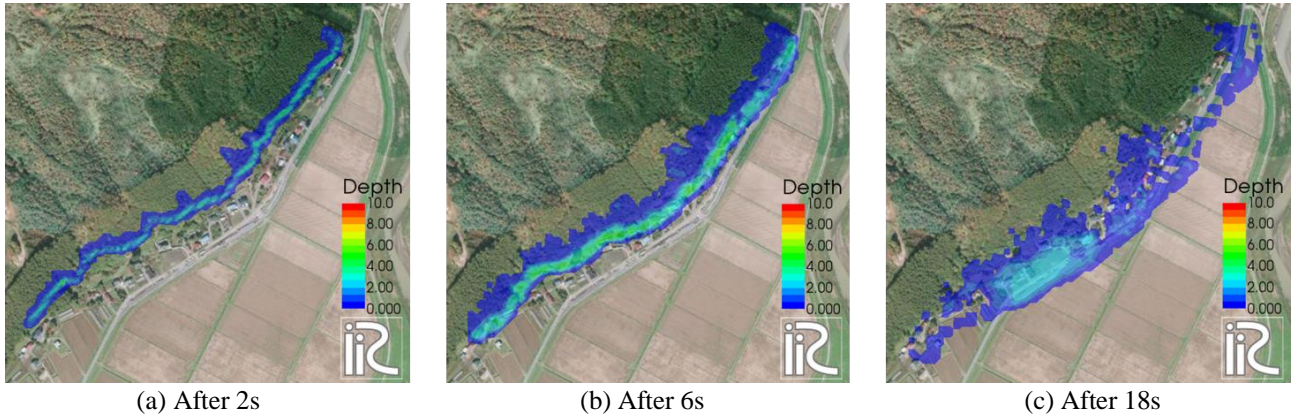
ξ and η are the coordinates in the flowing direction and the transverse direction in the general coordinate system, t is time, z is the water level, h is the surface flow depth, S_r is the water saturation, g is gravity, a_ξ , a_η , and a_z are accelerations due to the earthquake in ξ , η , and z directions, respectively, and θ is the bed slope of flow direction. P is pressure, z_b is bed height, U and V are inverse variable velocity components in ξ and η directions, $\tau_{b\xi}$ and $\tau_{b\eta}$ are inverse variable tractive force components in ξ and η directions, a_z is the seismic acceleration component in z direction. a_ξ and a_η are the contravariant seismic acceleration components in the ξ and η directions.

2.2 Yoshino area

The target area of this study is located in the Iburi district in southwestern Hokkaido. The Yoshino area is about 4 km northeast of the center of Atsuma city. The average annual rainfall is about 1000 mm, which is much lower than the Japanese national average. In the last 150 years, no major sediment disaster has occurred in the area.

3. DISCUSSION OF SIMULATION RESULTS

Fig. 1 shows the temporal change in the depth of the mud flow. The mud flow flows down the slope with increasing scale over time, and reaches the house in about 6 seconds. In addition, the depth when reaching the house is about 6 m: the mud flow can approach to the 2nd floor. The average velocity of the mud flowing down the slope is 13.5m/s. The mud flow spread over farmland. It is difficult to evacuate after the occurrence of the mud flow, considering that this mud flow originated from the earthquake, and the mudflow reached the residential land in short time after the slope failures are occurred. Therefore, it is important to avoid as much as possible to build houses near slopes with topsoil composed of fine-grained pyroclastic fall materials with high moisture retention.



(a) After 2s (b) After 6s (c) After 18s
Figure 1. Temporal change of mud flow depth in Yoshino area in numerical simulation (unit: m)

4. CONCLUSIONS

In Atsuma, Hokkaido, mud flow occurred due to the 2018 Hokkaido Eastern Iburi Earthquake. So, we conduct a numerical simulation of mud flow to discuss the flow characteristics of the mud flow due to Hokkaido Eastern Iburi Earthquake. The results showed that simulation was performed with high accuracy about flow range. In this case, the average velocity of the mud flowing down the slope is very fast, and reaches the house in about 6 seconds, so it is important to avoid as much as possible to build houses near slopes with topsoil composed of fine-grained pyroclastic fall materials with high moisture retention.

REFERENCES

Takebayashi H., Fujita, M. (2020). Numerical Simulation of a Debris Flow on the Basis of a Two-Dimensional Continuum Body Model. *Geosciences*, 10, 45.